Resonant ultrasound spectroscopy of $KTa_{1-x}Nb_xO_3$ ferroelectric relaxor crystals

O. Svitelskiy* and A. V. Suslov
National High Magnetic Field Laboratory, Florida State University, Tallahassee, Florida 32310, USA

J. B. Betts and A. Migliori
Los Alamos National Laboratory, Los Alamos, New Mexico 87545, USA

G. Yong
Towson University, Baltimore, Maryland 21252, USA

L. A. Boatner
Center for Radiation Detection Materials and Systems, Oak Ridge National Laboratory, Oak Ridge, Tennessee 37831, USA

(Received 14 April 2008; revised manuscript received 11 July 2008; published 20 August 2008)

The influence of the development of a ferroelectric state on the elastic properties of $KTa_{1-x}Nb_xO_3$ relaxor crystals is explored. The high sensitivity of the elastic stiffness tensor to the polar distortions and their reorientational dynamics is individual for each particular component: c_{11} and c_{44} are primarily influenced by the reorientational motion of the distortions between the nearest neighboring (111) directions; the c_{12}, however, depends primarily on the reorientations between the (111) directions neighboring along the cubic face diagonal. Consequently, the temperature behavior of c_{12} demonstrates a different dependence on the Nb concentration than that of c_{11} and c_{44}. In the 1.2% Nb crystal all three elastic coefficients clearly show a softening with the appearance of the dynamic polar distortions while, in the 16% Nb crystal this effect is strong for c_{11} and c_{44}, but changes in c_{12} occur only in the vicinity of the phase transition. Nevertheless, close to the transition the elastic properties become more isotropic for all three crystals. The curves of slowness and Young's modulus within the main crystallographic planes are presented and the linear compressibility modulus is estimated. The values of the Debye temperatures with an error of ± 2 K are estimated to be approximately 594, 589, and 592 for the crystals containing 1.2, 8, and 16% of Nb, respectively.

DOI: 10.1103/PhysRevB.78.064113 PACS number(s): 77.84.Dy, 77.80.−e, 62.20.de, 62.65.+k

I. INTRODUCTION

Relaxor ferroelectric compounds, especially the lead-based ones (e.g., $PbMg_{1/3}Nb_{2/3}O_3$, $PbZn_{1/3}Nb_{2/3}O_3$), are of essential importance for industrial applications as materials for memory elements, sensors, and actuators.[1,2] However, many aspects of the relaxor ferroelectricity phenomenon still remain unclear.[2–6] The reason for this is an extremely high complexity of the lead relaxors, in which the ionic displacement disorder is combined with complicated local structural and compositional disorder. Presence of the regions with face-centered symmetry in their cubic lattice makes analysis even more difficult.[7–9] Willing to shed more light on the nature of the relaxor phenomenon we feel that it is useful to concentrate on much simpler types of compounds, such as $KTa_{1-x}Nb_xO_3$ (KTN),[10] in which ferroelectricity is caused by off-centering of only one type of ion,[11] Nb. Similar to the lead relaxors, KTN has a perovskite lattice structure, where tantalum and niobium ions interchange in the centers, potassium ions occupy the corners, and oxygen ions are placed on the faces of the cubic cells. When the temperature is sufficiently high, the KTN crystal is paraelectric with cubic lattice symmetry. With cooling down, it undergoes a sequence of ferroelectric phase transitions to tetragonal (at T_{c1}), to orthorhombic (at T_{c2}), and finally to rhombohedral (at T_{c3}) symmetry.[12] If the concentration of Nb is small (between ~0.8 and 6%), only one transition is present, and at T_{c1}, the KTN crystal transforms from cubic to rhombohedral symmetry directly.[12] By changing the Nb concentration, one can vary the temperatures of the phase transitions. If the concentration of Nb is not too high ($\lesssim$30%) there is a strong influence of the relaxor behavior on the material properties.[13,14] This behavior is attributed to the appearance of the so-called polar nanoregions (PNRs), i.e., areas with ordered elementary electric dipole moments of the lattice cells,[15] which appear well above[16,17] T_{c1}. These are capable of a reorientational motion as single units; however on lowering the temperature, with each successive phase transition, their dynamics becomes progressively restricted until, in the rhombohedral phase, they are essentially frozen in a specific (111) direction.[18]

In this work we explore the influence of the PNRs on the KTN elastic properties using the high sensitivity of the method of resonant ultrasound spectroscopy[19] (RUS), in which from the spectrum of acoustical resonances the full elastic tensor of the crystal is derived. To the best of our knowledge, there are no publications presenting the temperature dependence of the full elastic tensor for any of the ferroelectric relaxor crystals. However, the analysis of temperature dependences of longitudinal[20,21] and transverse[21] acoustic phonons in the cubic phase of KTN (Ref. 21) and $PbMg_{1/3}Nb_{2/3}O_3$ (Refs. 22–24) single crystals suggests a strong coupling between phonons and PNRs. Application of RUS allows us to calculate simultaneously the full set of the elastic coefficients integrated over the whole crystal, to determine their temperature dependence, and to make a further step in understanding the coupling between the dynamic PNRs and sound waves.

TABLE I. Parameters of the investigated KTN crystals.

Nb (%)	Dimensions (mm)	Weight (grams)	Critical T (*K*)		
			T_{c1}	T_{c2}	T_{c3}
1.2	6.09×6.80×11.99	3.359	10		
8	4.82×5.05×9.08	1.509	90	84	76
16	5.11×9.18×11.41	3.565	135	125	110

II. EXPERIMENT

The method of RUS is based[19] on determining the resonance frequencies of the investigated object. For this purpose, the investigated sample is suspended in a cryostat almost freely between two transducers, so that the mechanical contact between the sample and each of the transducers is very weak. One of the transducers is used as a transmitter of the exciting ultrasound signal while another one serves as a receiver. If the excitation frequency is far away from any of the resonance frequencies of the investigated sample, then the receiving transducer does not detect any signal. If the excitation frequency is close to one of the resonances of the sample, then a strong sample vibration creates a signal at the receiving transducer. Having recorded the spectrum consisting of a set of resonances and knowing the mass, shape, and lattice structure of the sample, its full elastic stiffness tensor can be evaluated.[19] Repeating this procedure at different temperatures, the temperature dependence of the tensor can be obtained.

In the present work we have used three rectangular (100)-cut KTN crystals with Nb concentrations of 1.2%, 8%, and 16%. The surfaces of the crystals were polished to optical quality. The main parameters of these three specimens are summarized in Table I.

For each crystal, in a broad temperature range starting from room temperature and ending well below the temperature of the lowest phase transition, a set of spectra containing the first 40–45 resonances was recorded. Figure 1 shows examples of these spectra measured at several temperatures as the 8% KTN crystal approaches the first phase transition. When the temperature is well above T_{c1}, a typical spectrum consists of a number of strong and clearly identifiable resonances whose frequency depends on the temperature (see the spectra measured at 138.6 and 102.6 K). On approach to T_{c1}, with appearance of the PNRs, the spectrum becomes noisy (compare the spectra measured at 102.6 and 92.7 K). At T_{c1} this noise strengthens dramatically. Yet, the nucleation of the polar domains causes significant modifications in the spectrum because the resonance frequencies are defined not only by the sample mass and geometry, but also by the domain structure. The lack of a model capable to account for an effect of the domains on the sample vibrational spectrum does not allow us to perform the analysis below T_{c1}. Consequently, we have to limit our study to the lattice dynamics in the cubic phase (above T_{c1}) only.

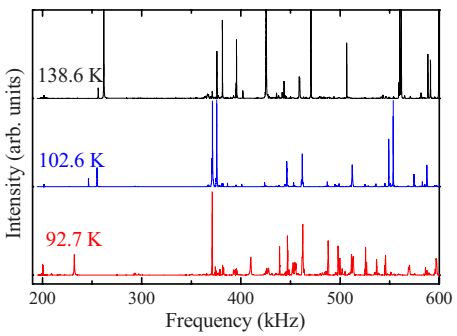

FIG. 1. (Color online) Examples of the acoustical resonance spectra of the 8% KTN crystal, measured at a number of different temperatures, as the sample approaches phase transition at T_{c1} ~90 K. The curves are offset for clarity.

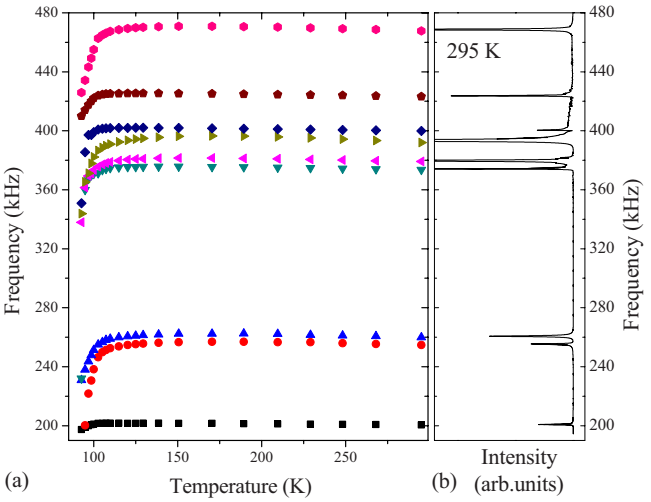

FIG. 2. (Color online) Example of the KTN crystal containing 8% of Nb: (a) frequencies of the first nine acoustical resonances as a function of temperature; (b) general look of the spectrum.

Figure 2(a) shows an example of the temperature dependences of the first nine resonances in the 8% KTN sample. To facilitate understanding, Fig. 2(b) also shows the spectrum of these resonances, measured at the room temperature.

III. ANALYSIS AND DISCUSSION

Assume, the elastic waves in the crystal have harmonic time dependence, i.e., $\sim e^{i\omega t}$. Their propagation is described by equation[19]

$$\rho\omega^2 u_l + \sum_{i,j,k,l} c_{ijkl}\frac{\partial^2 u_k}{\partial x_j\,\partial x_l} = 0 \qquad (1)$$

with the free-surface boundary conditions

$$\sum_j \vec{n}_j \sigma_{ij} = 0. \qquad (2)$$

Here ρ is the mass density, ω is the angular frequency, u_i and x_i are the i-th components of the displacement vector and Cartesian coordinate, c_{ijkl} is the $ijkl$-th component of the elastic stiffness tensor, and σ_{ij} is the ij-th component of the stress tensor. The indices i,j,k, and l run over all three spatial directions.

It is well known that a cubic symmetry lattice is characterized by three independent components of the elastic stiff-

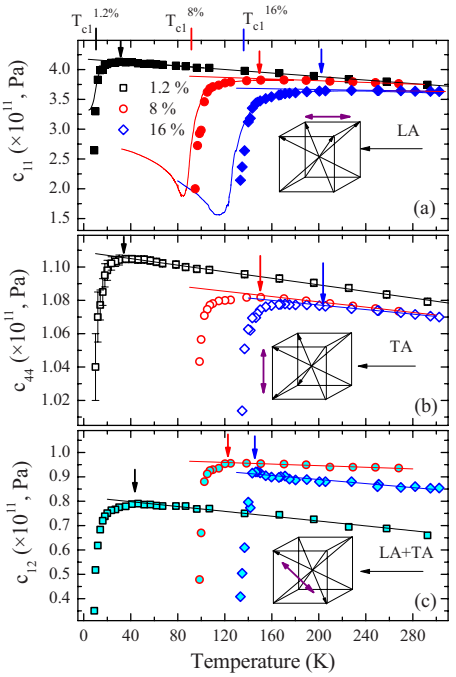

FIG. 3. (Color online) Temperature evolution of the elastic coefficients (a) c_{11}, (b) c_{44}, and (c) c_{12} calculated from the resonance spectra for the KTN crystals containing 1.2% (squares), 8% (circles), and 16% (diamonds) of Nb; solid curves in the panel (a) show corresponding c_{11} coefficients measured by the pulse-echo technique. The error, shown for c_{44} of 1.2% Nb crystal (b), is of the same relative magnitude for all calculated coefficients. Values of T_{c1} are shown on the top of the panel (a). Arrows mark the temperatures (± 5 K) at which the elastic coefficients deviate from straight lines.

ness tensor.[25] Using the Voight notation, there are c_{11}, related to the longitudinal acoustic (LA) wave propagating in (100) direction, c_{44}, related to the transverse acoustic (TA) wave propagating in (100) and polarized in (010) direction, and c_{12}, which by itself does not control any sound wave, but the difference $(c_{11}-c_{12})$ describes, for example, a shear wave propagating in (011) and polarized in (100) direction. Figure 3 shows the temperature dependences of these quantities determined by numerically solving Eqs. (1) and (2) using the measured values of the resonance frequencies. Small at high temperatures, the error of calculations significantly increases on approach to T_{c1}, as shown with error bars on the example of c_{44} for the crystal with 1.2% of Nb [Fig. 3(b)]. To double-check that the solution converged to the correct values, one of the coefficients, c_{11}, was also measured by the conventional ultrasonic pulse-echo technique[26] using 40-MHz transducers [solid lines in Fig. 3(a)]. The close agreement between the c_{11} values, obtained by the two different methods is remarkable. A small mismatch on close approach to T_{c1} is caused by an increasing uncertainty in both the RUS and pulse-echo measurements due to the growing influence of the randomly oriented dynamic PNRs with tetragonal local symmetry. In these conditions, the elastic coefficients lose their genuine meaning, which is accompanied by the deviation of the frequencies of the resonances in the RUS method, and dissipation of the ultrasonic signal and deterioration of the pulse shapes in the pulse-echo method. The results for c_{11} and c_{44} are also in agreement with the earlier works.[20,21]

At a glance, on all samples the three elastic coefficients demonstrate similar trends in their behavior (Fig. 3). Starting from high temperature, the coefficients initially show a usual linear increase. However with further cooling they deviate from straight line (the deviation points are marked with arrows) and start to soften—at first slowly and subsequently with increasing speed. This softening, being precursor to the transition, is related to appearance of dynamic PNRs capable of reorientational motion and their interaction with phonons[21–24] and represents a consequence of relaxor behavior. Close to T_{c1} the softening turns into a sharp decrease.

A closer examination of Fig. 3 reveals an interesting feature. In the 1.2% Nb crystal the deviation of c_{11} and c_{44} starts much closer to the transition temperature than in two other crystals, as it is expected from the earlier study,[20] where on approach of the KTN composition to pure $KTaO_3$, a gradual disappearance of $1/s_{11}$ softening was observed (s_{11} is elastic compliance coefficient). However, the c_{12} coefficient behaves differently: its deviation starts 40 ± 5 degrees above T_{c1} for the 1.2% sample, 25 ± 5 degrees for the 8% sample, and 10 ± 5 degrees for the 16% sample, as marked with arrows in Fig. 3(c), so the c_{12} decrease becomes sharper with increase in Nb concentration. This observation reflects the fact that c_{11}, c_{44}, and c_{12} couple to different types of reorientational motion of the PNRs through their interaction with the LA, TA, and mixture of LA and TA waves, respectively. While the c_{11} and c_{44} are sensitive to the librations of PNRs between the neighboring (111) directions,[21] c_{12} is more susceptible to the reorientations of PNRs between the (111) directions, located over the face diagonal, as illustrated in insets in Fig. 3. The last type of reorientational motion is the most sensitive to increase in Nb concentration. When the concentration is small, the face diagonal motion of the PNRs is plausible, and through coupling to the acoustic waves, it influences the c_{12} coefficient [Fig. 3(c)] by deviating it from the linear dependence at temperatures that are significantly higher than T_{c1} (the 1.2% case). The increase in Nb concentration causes the growth of the PNR sizes and fixes their orientation along one of the (100) directions.[18] Consequently, the face diagonal reorientations become less favorable, and the c_{12} coefficient continues to follow a linear dependence until the temperature is very close to T_{c1} (i.e., the 16% Nb case).

With further growth of Nb concentration, at $\gtrsim 50\%$, the KTN crystal loses its relaxor properties and behaves as a classical ferroelectric.[13] In our opinion, in this case the elastic coefficients at the phase transition should exhibit a sharp discontinuity, such as[27] in $BaTiO_3$ or $PbTiO_3$. In effect, further increase in Nb content should reduce precursor softening of c_{11} and c_{44} down to its total disappearance.

Obtained experimental data allow us to determine a number of fundamental parameters of the material that are important for building experimental devices, e.g., microactuators and other microelectromechanical systems (MEMS), and for theoretical simulations of the KTN properties—in particular, for first-principles calculations.[28,29] Using the Christoffel equations, one can calculate the value of the sound speed in an arbitrary direction:[30]

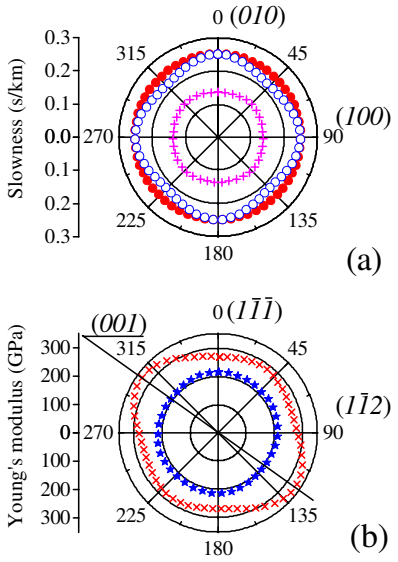

FIG. 4. (Color online) Example of the KTN crystal containing 16% of Nb: (a) room temperature (100) plane cross-sections of the slowness surfaces (solid and open circles stay for the shear and quasishear modes, crosses represent the quasilongitudinal mode); (b) (110) plane cross sections of the Young's modulus surface calculated at the room temperature (crosses) and at 136 K (stars).

$$(c_{ijkl}K_jK_l - \rho v^2\delta_{ik})U_k = 0, \tag{3}$$

where K_i, U_j are the direction cosines for propagation and polarization vectors; δ_{jk} is the Kronecker symbol. As an example, the (100) plane cross-sections of the room temperature slowness (reciprocal speed) surfaces calculated for the KTN sample containing 16% of Nb are shown in Fig. 4(a).

It is also straightforward to determine the Young's modulus,[25] the ratio of an applied longitudinal stress to the resulting longitudinal strain. The anisotropy of the modulus is demonstrated in Fig. 4(b). The development of the PNRs changes its shape dramatically. While at the room temperature the Young's modulus extends along (001) direction [Fig. 4(b)], near the phase transition it is almost isotropic with a weak elongation along (111) direction. This is the consequence of the fundamental change in the anisotropy factor[30] of the sample $A=2c_{44}/(c_{11}-c_{12})$ from $A=0.77<1$ at room temperature to $A=1.08\gtrsim 1$ on approach to T_{c1}.

Another important characteristic of the crystal is its linear compressibility. In the cubic system, its value is isotropic and at room temperature equals to about 1.9 ± 0.1 T Pa^{-1} for all crystals. On approach to T_{c1}, starting from 10–20 degrees above T_{c1} this value increases up to about 3 T Pa^{-1}.

The Debye temperature of a KTN crystal can be estimated from[31]

$$\Theta_D = \frac{\hbar}{k_b}\left(\frac{6\pi^2 N}{V}\right)^{1/3} v_D,$$

$$v_D^{-3} = \frac{1}{12\pi}\sum_{i=1}^{3}\int_{\Omega} v_i^{-3}(\theta,\varphi)d\Omega, \tag{4}$$

where $\hbar$ and k_b are the Planck and Boltzmann constants, N is the number of atoms in a unit cell, and V is the volume of the unit cell. Calculating the average velocity v_D, the summation runs over all three angle θ- and φ-dependent acoustic phonon modes, and the integration runs over the whole solid angle Ω of 4π. For the 16% Nb KTN crystal at room temperature the ratio $N/V\approx 7.9\times10^{22}$ atoms/cm^3. The average speed of sound is $v_D\approx 4.67$ km/sec so the value of the Debye temperature[31] is $\Theta_D\approx 592\pm2$ K. Similar calculations for the 1.2 and 8% Nb crystals yield 594 ± 2 and 589 ± 2 K, respectively. These estimates complement the older value of $\Theta_D\sim 580$ K,[32] obtained for the quantum ferroelectric $KTaO_3$ crystal.

As a final note, strong noises due to the multiple scattering on the domain walls did not allow us to extend this exploration to the lower-symmetry phases. To overcome the problem, ultrasonic experiments involving poling the crystals are necessary. Alternatively, the elastic coefficients can be determined from micro-Brillouin scattering spectra, as it was done, e.g., in Ref. 33. While the ultrasonic methods probe macroscopic properties of the crystal as a whole, the micro-Brillouin scattering retrieves information from microregions in the crystal.

IV. SUMMARY

Using the method of RUS, we have explored the influence of the PNRs on the KTN elastic properties during the development of the ferroelectric state. All three independent elastic coefficients show a high sensitivity to the appearance of the polar distortions, but they interact with the PNRs motion differently. While the c_{11} and c_{44} are strongly influenced by the PNRs reorientations between the nearest neighboring (111) directions, the c_{12} value is mainly sensitive to reorientations between the (111) directions neighboring along the face diagonal. Consequently, in our range of concentrations the c_{12} softening strongly depends on the Nb concentration and exhibits narrowing of its relaxor temperature range when this concentration increases. Being connected directly with size distribution and temperature evolution of the PNRs and their interaction with phonons, a similar effect is also expected for c_{11} and c_{44} coefficients. From the elastic coefficients, a number of fundamental KTN parameters were evaluated including the velocity of the arbitrary sound wave, the Young's modulus, the linear compressibility, and the Debye temperature. Near the phase transition ($T\approx T_{c1}+2$ K) the elastic anisotropy factor approaches unity and the crystals are practically isotropic in terms of elasticity.

ACKNOWLEDGMENTS

Authors are thankful to Scott Headley for helping with the experimental setup. The experiment has been performed at the NHMFL, which is supported by the NSF Cooperative Agreement No. DMR-0084173 and the State of Florida. The ultrasonic research at the NHMFL is supported by the In-House Research Program. Research at ORNL is sponsored by the Division of Materials Sciences and Engineering, Office of Basic Energy Sciences, U.S. Department of Energy, under Contract No. DE-AC05-00OR22725 with Oak Ridge National Laboratory, managed and operated by UT-Battelle, LLC.

*Present address: Department of Physics, University of Alberta, Edmonton, Alberta T6G 2G7, Canada

[1] O. Auciello, J. F. Scott, and R. Ramesh, Phys. Today **51**(7), 22 (1998).
[2] Z. Kutnjak, J. Petzelt, and R. Blinc, Nature (London) **441**, 956 (2006).
[3] G. Shirane, G. Xu, and P. M. Gehring, arXiv:cond-mat/0306183, Ferroelectrics **321**, 7 (2005).
[4] Z. G. Ye, Key Eng. Mater. **155-156**, 81 (1998), and references therein.
[5] E. V. Colla, M. B. Weissman, P. M. Gehring, Guangyong Xu, Haosu Luo, P. Gemeiner, and B. Dkhil, Phys. Rev. B **75**, 024103 (2007), and references therein.
[6] O. Svitelskiy, D. La-Orauttapong, J. Toulouse, W. Chen, and Z. G. Ye, Phys. Rev. B **72**, 172106 (2005), and references therein.
[7] J. Chen, H. M. Chan, and M. P. Harmer, J. Am. Ceram. Soc. **72**, 593 (1989).
[8] I.-K. Jeong, T. W. Darling, J. K. Lee, Th. Proffen, R. H. Heffner, J. S. Park, K. S. Hong, W. Dmowski, and T. Egami, Phys. Rev. Lett. **94**, 147602 (2005).
[9] M. A. Akbas and P. K. Davies, J. Am. Ceram. Soc. **83**, 119 (2000).
[10] G. Yong, J. Toulouse, R. Erwin, S. M. Shapiro, and B. Hennion, Phys. Rev. B **62**, 14736 (2000).
[11] O. Hanske-Petitpierre, Y. Yacoby, J. Mustre de Leon, E. A. Stern, and J. J. Rehr, Phys. Rev. B **44**, 6700 (1991).
[12] D. Rytz and H. J. Scheel, J. Cryst. Growth **59**, 468 (1982).
[13] J. Toulouse and R. K. Pattnaik, Phys. Rev. B **65**, 024107 (2001).
[14] J. Toulouse and R. Pattnaik, Ferroelectrics **199**, 287 (1997).
[15] E. Bouziane and M. D. Fontana, J. Phys.: Condens. Matter **9**, 10249 (1997).
[16] J. Toulouse and R. K. Pattnaik, J. Phys. Chem. Solids **57**, 1473 (1996).
[17] P. DiAntonio, B. E. Vugmeister, J. Toulouse, and L. A. Boatner, Phys. Rev. B **47**, 5629 (1993).
[18] O. Svitelskiy and J. Toulouse, J. Phys. Chem. Solids **64**, 665 (2003), and references therein.
[19] A. Migliori and J. Sarrao, *Resonant Ultrasound Spectroscopy* (Wiley, New York, 1997); A. Migliori, J. L. Sarrao, W. M. Visscher, T. M. Bell, Ming Lei, Z. Fisk, and R. G. Leisure, Physica B (Amsterdam) **183**, 1 (1993).
[20] D. Rytz, A. Chantelain, and U. T. Hochli, Phys. Rev. B **27**, 6830 (1983).
[21] L. A. Knauss, X. M. Wang, and J. Toulouse, Phys. Rev. B **52**, 13261 (1995).
[22] N. K. Yushin and S. N. Dorogovtsev, Ferroelectrics **143**, 49 (1993).
[23] S. D. Prokhorova and S. G. Lushnikov, Ferroelectrics **90**, 187 (1989).
[24] R. Laiho, S. Lushnikov, and I. Siny, Ferroelectrics **125**, 493 (1992).
[25] J. F. Nye, *Physical Properties of Crystals* (Clarendon, Oxford, 1985).
[26] A. Suslov, B. K. Sarma, J. Feller, and J. Ketterson, Rev. Sci. Instrum. **77**, 035104 (2006).
[27] Z. Li, M. Grimsditch, C. M. Foster, and S. K. Chan, J. Phys. Chem. Solids **57**, 1433 (1996).
[28] S. A. Prosandeev, E. Cockayne, and B. Burton, First-principles calculations of ionic vibrational frequencies in PbMg1/3Nb2/303, in *Fundamental Physics of Ferroelectrics 2003*, edited by P. K. Davies and D. J. Singh, AIP Conf. Proc. No. 637, v. 146, (AIP, New York, 2003), p. 64.
[29] V. A. Trepakov, S. A. Prosandeev, M. E. Savinov, P. Galinetto, G. Samoggia, S. E. Kapphan, L. Jastrabik, and L. A. Boatner, J. Phys. Chem. Solids **65**, 1317 (2004).
[30] B. A. Auld, *Acoustic Fields and Waves in Solids* (Krieger, Malabar, FL, 1990), Vol. 1.
[31] G. Grimvall, *Thermophysical Properties of Materials* (North-Holland, Amsterdam, 1986).
[32] W. N. Lawless, Phys. Rev. B **16**, 433 (1977).
[33] M. Ahart, A. Asthagiri, P. Dera, H.-K. Mao, R. E. Cohen, and R. J. Hemley, Appl. Phys. Lett. **88**, 042908 (2006).